Figure 2. Isothermal plots of magnetic moment, σ, as a function of applied magnetic field, H. The sample is composed of small crystals of **2** as a pressed pellet.

of total moment $\sigma = N\gamma$ to occur at the critical field $H_c = \Delta/\gamma$. At finite T the transition will still be abrupt (although thermally broadened) provided that, at $H = H_c$, $T < \Delta/k \equiv T_N$. For $T > T_N$ the transition is thermally quenched and $\sigma = N\gamma \sinh(\gamma H/kT)/(1 + \cosh(\gamma H/kT))$ becomes a smooth function of H. It may be verified from eq 1 that the low-field slope, $(\partial\sigma/\partial H)_T$ ($T \rightarrow 0$ K), is predicted to increase with temperature for $T < T_N$. These features are in qualitative accord with the data of Figure 1 ($T_N = \Delta/k = 2.55$ K). Further development and consequences of the model will be published elsewhere.

This model, however, does not rule out the more conventional ideas of two magnetic lattices (one anti and the other ferromagnetic) coupled, but the model gives a surprisingly good fit of the data which is not possible within the conventional model.

Acknowledgment. The authors thank Drs. M. H. Cohen (Chicago), D. O. Cowan (Johns Hopkins), A. J. Epstein (Xerox), R. G. Munro (NBS), and C. Scott (Cornell) for helpful discussions.

References and Notes

(1) (a) Reis, A. H., Jr.; Preston, L. D.; Williams, J. M.; Peterson, S. W.; Candela, G. A.; Swartzendruber, L. J.; Miller, J. S. *J. Am. Chem. Soc.*, following paper in this issue. (b) Miller, J. S.; Reis, A. H., Jr.; Gebert, E.; Ritsko, J. J.; Salaneck, W. R.; Kovnat, L.; Cape, T. W.; van Duyne, R. P., *ibid.*, in press.
(2) (a) Jacobs, I. S.; Lawrence, P. E. *Phys. Rev.* **1967**, *164*, 866. Wilkinson, M. K.; Cable, J. W.; Wollan, E. O.; Koehler, W. C. *Ibid.* **1959**, *113*, 497. (b) Eichelberger, H.; Majeste, R.; Surgi, R.; Trefonas, L.; Good, M. L.; Karraker, D. *J. Am. Chem. Soc.* **1977**, *99*, 616. (c) Stryjewski, E.; Giordano, N. *Adv. Phys.* **1977**, *26*, 487.
(3) Hendrickson, D. N.; Sohn, Y. S.; Gray, H. B. *Inorg. Chem.* **1971**, *10*, 1559.
(4) Goldberg, I. B., unpublished results.
(5) (a) Wertheim, G. K.; Herber, R. H. *J. Chem. Phys.* **1963**, *38*, 2106. (b) Collins, R. L. *ibid.*, **1965**, *42*, 1072.
(6) (a) de Jonge, W. J. M.; van Vlimmeren, Q. A. G.; Hijmans, J. P. A. M.; Swuste, C. H. W.; Buys, J. A. H. M.; van Workum, G. J. M. *J. Chem. Phys.* **1977**, *67*, 751. (b) Foner, S.; Frankel, R. B.; Reiff, W. M.; Little, B. L.; Long, G. J. *Solid State Commun.* **1975**, *16*, 159.
(7) Address correspondence to Occidental Research Corporation, 2100 SE Main, Irvine, Calif. 92713.

G. A. Candela,* L. J. Swartzendruber

National Bureau of Standards, Department of Commerce
Washington, D.C. 20234

Joel S. Miller,*[7] M. J. Rice

Webster Research Center, Xerox Corporation
*Rochester, New York 14644*

Received November 17, 1977

Crystal and Molecular Structure of the Paramagnetic 1:1 Decamethylferrocenium 7,7,8,8-Tetracyano-*p*-quinodimethanide Dimer Salt: {[Fe(C₅Me₅)₂]⁺·}₂(TCNQ)₂²⁻

Sir:

In the past few years there has been an interest in the chemical and physical properties of the reaction products between inorganic complexes and 7,7,8,8-tetracyano-*p*-quinodimethane, TCNQ.[1,2] Such materials exhibit high electrical conductivity, unique structures, and in some cases unusual oxidation states. For example, 1:2 ferrocene complexes of TCNQ were first reported in 1962 to exhibit high electrical conductivity.[2] In order to understand the properties of this class of charge-transfer complexes and in particular to form a volatile complex (which permits the unique physical studies performed on tetrathiofulvalenium TCNQ,[3] (TTF)(TCNQ), to be extended), a series of new TCNQ complexes with decamethylferrocene, DMeFc, namely 1:1 paramagnetic (phase I), metamagnetic (phase II),[4] and a 1:2 salt were prepared. Herein we report the molecular and crystal structure of the paramagnetic 1:1 salt of decamethylferrocene and TCNQ, (DMeFc⁺·)₂(TCNQ)₂²⁻ (**1**).

The dark purple reflecting salt, **1**, which forms flat-plate crystals from 1:1 solutions of DMeFc and TCNQ in acetonitrile[5] upon standing for long periods of time, belongs to the monoclinic $P2_1/c$ (C_{2h}^5, No. 14) space group ($a = 9.7076$ (12), $b = 12.2113$ (17), $c = 23.5849$ (36) Å; $\beta = 95.012$ (2)°; $Z = 4$; and $\rho_{calcd} = 1.265$ g cm⁻³ ($\rho_{obsd} = 1.269$ g cm⁻³ by flotation in cyclohexane and 1,2-dibromoethane)). The structure was determined by a combination of Patterson, direct methods, Fourier, and least-squares refinement techniques to an $R_f = 0.058$ for the 3042 independent observable reflections ($F_{obsd} > \sigma F_{obsd}$) from a total of 3667 reflections collected on a Syntex P2₁ automated diffractometer to $2\theta \leqslant 45°$ (Mo K$\bar{\alpha}$).

The crystalline lattice consists of isolated units of Fe(C₅Me₅)₂/TCNQ/TCNQ/Fe(C₅Me₅)₂, i.e., dimers of A:B:B:A composition, Figure 1. This result differs from the donor–acceptor complexes reported for ferrocene tetracyanoethylene[6a] and phase I (DMeFc)(TCNQ)[4b] and proposed for ferrocene bis(arene)iron(II).[6b] This is probably due in part to the complete charge transfer in **1** and the tendency of TCNQ⁻· to dimerize. The A:B:B:A units do not form infinite 1-D chains as previously reported for Nb₃Cl₆(C₆Me₆)₃-(TCNQ)₂.[1b] Within each dimeric unit the DMeFc⁺· ion is oriented such that the two C₅ rings are parallel and directly above a (TCNQ⁻)₂ ion with the result that the C₁₃ of the TCNQ⁻· lies approximately in the center of the C₅ ring (Figure 1), and the interplanar distance between the C₅ ring and the TCNQ⁻· ion is 3.554 Å. Like Fc⁺·BiCl₄⁻ [7] the DMeFc⁺·
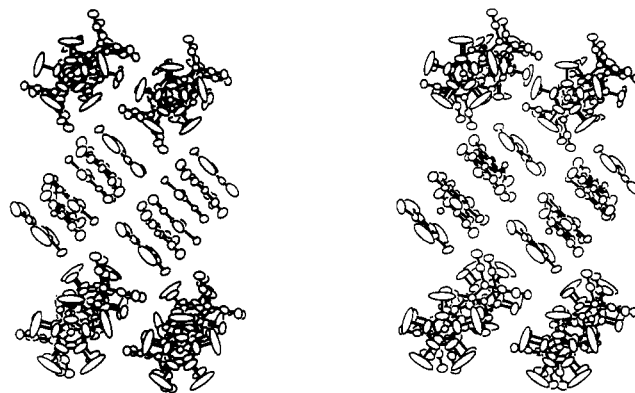
Figure 1. A stereoview of the parallel and perpendicular A:B:B:A (A = DMeFc⁺·; B = TCNQ⁻·) units within the TCNQ⁻· lattice. Half of the units which lie within the plane of the drawing have been omitted for clarity.
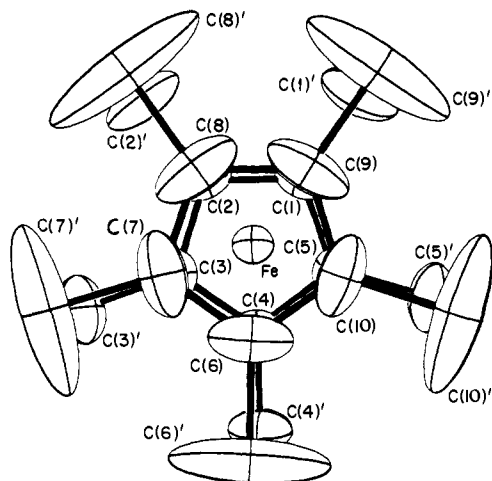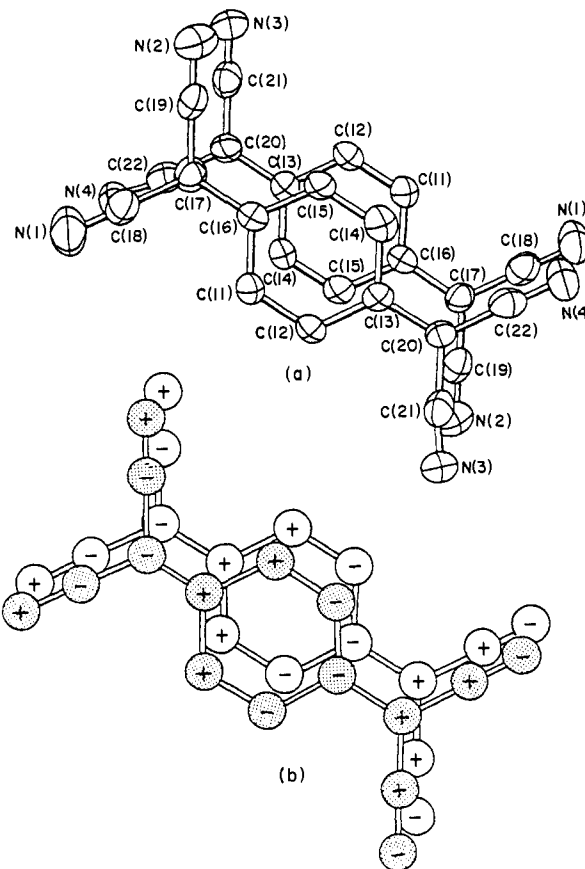
Figure 2. A view of the DMeFc⁺· ion down the C_5 rotation axis showing the eclipsed nature of the C_5 ring and the ordered and disordered C_5 rings.
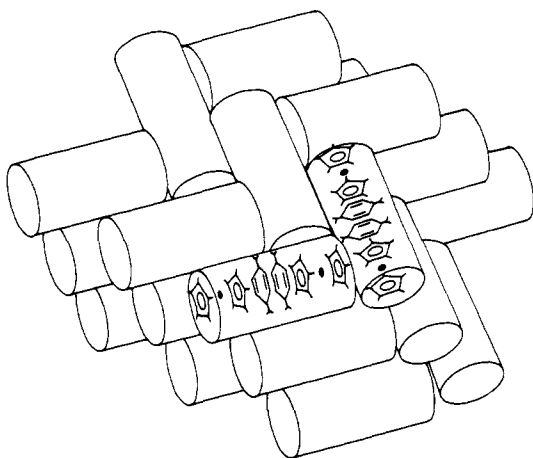
Figure 3. Schematic illustration of the crystal structure of (DMeFc⁺·)$_2$-(TCNQ)$_2{}^{2-}$. Each cylinder represents a dimer.

Figure 4. (a) The (TCNQ)$_2{}^{2-}$ dimeric unit showing the offset of one ion. (b) Overlap of the bonding a_u dimer orbital. The a_u orbital arises from overlap of the POMO b_{2g} orbitals on each TCNQ⁻· ion. The signs of the wavefunctions on the top TCNQ⁻· (dark line) refer to the underneath side of the π lobes. The converse is true for the underneath TCNQ⁻· moiety.

Table I. Fe—Fe and Fe—N Distances in (DMeFc⁺·)$_2$(TCNQ)$_2{}^{2-}$

symmetry position	distance, Å	symmetry position	distance, Å
A. Fe—Fe Interactions			
$2 - x$, $\frac{1}{2} + y$, $\frac{3}{2} - z$	7.882 (1)	$2 - x$, $1 - y$, $2 - z$	11.877 (2)
$2 - x$, $2 - y$, $2 - z$	8.802 (1)	x, $\frac{3}{2} - y$, $\frac{1}{2} + z$	12.077 (2)
$1 + x$, y, z	9.708 (1)	x, $1 + y$,z	12.211 (2)
$1 - x$, $\frac{1}{2} + y$, $\frac{3}{2} - z$	9.843 (1)	$1 - x$, $1 - y$, $2 - z$	13.993 (2)[a]
$1 - x$, $2 - y$, $2 - z$	11.499 (2)		
B. Fe—NC Interactions (<6 Å)			
N(2), $1 - x$, $\frac{1}{2} + y$, $\frac{3}{2} - z$	5.363		
N(2), $1 + x$, $\frac{3}{2} - y$, $\frac{1}{2} + z$	5.412		
N(4), $1 - x$, $2 - y$, $1 - z$	5.431		
N(1), x, y, z	5.539		

[a] Intradimer spacing.

ion has an eclipsed C_5 ring configuration (Figure 2), whereby one of the C_5 rings, which is parallel and stacked on an adjacent TCNQ⁻· ion, shows no disorder, normal anisotropic thermal ellipsoids, and distinct methyl-hydrogen positions. The other C_5 ring, which is adjacent to an orthogonal tetradic unit (Figures 1 and 3) shows disorder about the C_5 axis, large thermal ellipsoids, and no methyl-hydrogen positions. The average Fe-C, C-C, and C-Me distances are 2.090 (7), 1.400 (7), and 1.515 (9) Å, respectively. Each Fe(III) atom is completely encased by the negatively charged C_5 rings and N atoms of several TCNQ⁻· ions. (Table I gives the closest Fe·· ·NC interactions). The TCNQ⁻· dimer is offset along the short molecular axis in a manner that allows nominal b_{2g} overlap and a short interplanar spacing of 3.147 Å (Figure 4). This type of slippage has been observed for many materials containing TCNQ⁻· dimers, e.g., Rb(TCNQ),[8a] Cs$_2$(TCNQ)$_3$,[8b] and (morpholinium)$_2$(TCNQ)$_3$.[8c] This close approach is similar to the slipped exo-ring TCNQ⁻· overlap observed in Nb$_3$Cl$_6$(C$_6$Me$_6$)$_3$(TCNQ)$_2$[1b] in that the electron density residing on the cyano groups forces the CN ligands to bend away from the TCNQ plane in a direction away from the dimer centroid and toward the nondisordered C_5 ring.

The C(16)-C(17) and C(13)-C(20) bond lengths (Figure 4) in TCNQ⁻· have been used to determine the apparent charge on the TCNQ molecule.[1a,8a,9] In DMeFc⁺·TCNQ⁻· these distances are 1.418 (6) and 1.402 (6) Å, respectively, and are consistent with a full negative charge on the TCNQ⁻· ion. Therefore, the DMeFc⁺· ion contains Fe(III). This is in accord with the Mössbauer data which shows a slightly asymmetric singlet with an isomer shift of 0.42 mm s⁻¹ (78 K with respect

to iron metal at 298 K) characteristic of $S = \frac{1}{2}$ Fe^{III}.[4a] The average Fe-C bond distance of 2.090 (7) Å[10] (0.05 ± 0.01 Å longer than in ferrocene[11]) is in part indicative of a less covalently bonded η^5-C$_5$-Fe-η^5-C$_5$ unit. This is consistent with the ionic manganocene[12] since Fe(III) is isoelectronic with Mn(II). However, the eclipsed C_5 methyl groups of DMeFc⁺· will cause the C_5 rings to be separated more than in the ferrocene; so the

amount of ionic character in the Fe–C bond is at this time undetermined.

The magnetic susceptibility of powder samples of **1**, in contrast to the 1-D polymorph, obeys the Curie expression, i.e., $\chi T = 0.81$ BM. This is in accord with values obtained for other ferrocenium salts[13] and suggests very little magnetic coupling between the intradimer $S = \frac{1}{2}$Fe(III)'s separated by ~ 14 Å. The $(TCNQ)_2{}^{2-}$ dimer is strongly antiferromagnetically coupled. For single crystals of **1**, $\chi_{\parallel} = 2\chi_{\perp}$ where $\chi_{\parallel}$ is measured parallel to the dimer axis. In **1** the structural arrangement consists only of isolated dimers. Within an isolated dimer the $S = \frac{1}{2}$Fe^{III} sites are 13.993 (2) Å apart and the separation between DMeFc^{+}· and TCNQ^{-}· (3.554 Å) and TCNQ^{-}·– TCNQ^{-}· (3.147 Å) suggest that b_{2g}–b_{2g} electronic interactions exist within the dimer to form a filled a_u bonding orbital (Figure 4b). Coupling between parallel and perpendicular dimers appears to be minimal owing to a lack of direct orbital interactions; however, cyano interactions with the DMeFc^{+}· ion where N(4) has a close approach of 3.271 Å to C(8)′ and 3.354 Å to C(2)′ suggest some interactions. Also, there are numerous Fe^{III}–Fe^{III} distances (Table I), which are significantly shorter than the intradimer Fe–Fe distance.

References and Notes

(1) E.g., see the following. (a) Goldberg, S. Z.; Eisenberg, R.; Miller, J. S.; Epstein, A. J. *J. Am. Chem. Soc.* **1976**, *98*, 5173. (b) Goldberg, S. Z.; Spivack, B.; Stanley, G.; Eisenberg, R.; Braitsch, D. M.; Miller, J. S.; Abkowitz, M. *ibid.* **1977**, *99*, 110. (c) Endres, H.; Keller, H. J.; Moroni, W.; Nothe, D. *Z. Naturforsch. B.* **1976**, *31*, 1322. (d) Siedle, A. R. *J. Am. Chem. Soc.* **1975**, *97*, 5931. (e) Miles, M. G.; Wilson, J. D. *Inorg. Chem.* **1975**, *14*, 2357. (f) Shibaeva, R. B.; Atovmyan, L. O.; Orfanova, M. N. *Chem. Commun.* **1969**, 1494. (g) Williams, R. M.; Wallwork, S. C. *Acta Crystallogr., Sect. B* **1968**, *24*, 168.
(2) Melby, L. R.; Harder, R. J.; Hertler, W. R.; Mahler, W.; Benson, R. E.; Mochel, W. E. *J. Am. Chem. Soc.* **1962**, *84*, 3374.
(3) Engler, E. M. *Chem. Tech.* **1976**, *6*, 274. Andre, J. J.; Bieber, A.; Gaultier, F. *Ann. Phys.* **1976**, *1*, 145. Berlinsky, A. J. *Contemp. Phys.* **1976**, *17*, 331.
(4) (a) Candela, G. A.; Swartzendruber, L.; Miller, J. S.; Rice, M. J. *J. Am. Chem. Soc.*, preceding paper in this issue. (b) Miller, J. S.; Reis, A. H., Jr.; Gebert, E.; Ritsko, J. J.; Salaneck, W. R.; Kovnat, L.; Cape, T. W.; Van Duyne, R. P. *ibid.*, in press.
(5) Ritsko, J. J.; Nielsen, P.; Miller, J. S. *J. Chem. Phys.*, **1977**, *67*, 687.
(6) (a) Adman, E.; Rosenblum, M.; Sullivan, S.; Margulis, T. N. *J. Am. Chem. Soc.* **1967**, *89*, 4540. (b) Braitsch, D. M. *J. Chem. Soc., Chem. Commun.* **1976**, 460.
(7) Mammano, N. J.; Zalkin, A.; Landers, A.; Rheingold, A. L. *Inorg. Chem.* **1977**, *16*, 297.
(8) (a) Hoekstra, A.; Spoelder, T.; Vos, A. *Acta Crystallogr., Sect. B* **1972**, *28*, 14. (b) Fritchie, C. J., Jr.; Arthur, P., Jr. *Acta Crystallogr.* **1966**, *21*, 139. (c) Sundaresan, T.; Wallwork, S. C. *Acta Crystallogr., Sect. B* **1972**, *28*, 491.
(9) Herbstein, F. H. *Perspect. Struct. Chem.* **1971**, *4*, 166.
(10) This is similar to the 2.10-Å Fe–C separation in Fe(C$_5$H$_5$)$_2$I$_3$: Bernstein, T.; Herbstein, F. H. *Acta Crystallogr., Sect. B* **1968**, *24*, 1640.
(11) Dunitz, J. D.; Orgel, L. E.; Rich, A. *Acta Crystallogr.* **1956**, *9*, 373.
(12) Cotton, F. A.; Wilkinson, G. "Advanced Inorganic Chemistry", Interscience: New York, 1972; p 743.
(13) Hendrickson, D. N.; Sohn, Y. S.; Gray, H. B. *Inorg. Chem.* **1971**, 10, 1559.
(14) Participant in the Undergraduate Research Participation Program sponsored by the Argonne Center for Educational Affiars from Knox College, Galesburg, Ill.
(15) Work performed under the auspices of the Division of Physical Research of the U.S. Energy Research and Development Administration.
(16) Address correspondence to Occidental Research Corp., 2100 SE Main, Irving, Calif. 92713.

A. H. Reis, Jr.,* L. D. Preston[14]
J. M. Williams, S. W. Peterson

Chemistry Division, Argonne National Laboratory
Argonne, Illinois 60439[15]

G. A. Candela, L. J. Swartzendruber

National Bureau of Standards, Department of Commerce
Washington, D.C. 20236

Joel S. Miller*[16]

Webster Research Center, Xerox Corporation
*Rochester, New York 14644*

Received November 17, 1977

Spin Trapping of Adsorbed Hydrogen

Sir:

The spin trapping technique has been widely used to identify radical species produced in solution or the gas phase.[1] The method has not hitherto been applied to species adsorbed from the gas phase on solid catalyst surfaces. We report in this communication the scavenging of hydrogen adsorbed on zinc oxide by the spin trap *N-tert*-butyl-α-phenylnitrone (PBN, **I**).

$$\underset{\text{I}}{PhCH{=}\overset{O^-}{\underset{}{N^+}}C(CH_3)_3}$$
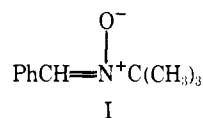
PBN has been used to trap radicals produced during radiolysis of liquid hydrocarbons,[2] irradiation of gaseous CO–H$_2$ mixtures,[3] and electrolysis of water.[4] A radical R· will attack

$$\underset{\text{II}}{Ph\overset{H}{\underset{R}{C}}{-}\overset{O\cdot}{N}C(CH_3)_3}$$
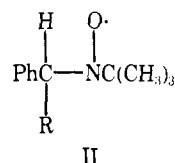
the α carbon of **I** to produce the stable radical **II**, and the nature of R· may be deduced from the EPR spectrum of **II**.

Zinc oxide samples (Kadox, 5 m^2 g^{-1}) were outgassed in vacuo at 400 °C and then exposed to H$_2$ or D$_2$ at room temperature for 10 min. After brief evacuation, a solution of PBN in benzene (4×10^{-3} N) was added to the sample through a grease-free stopcock. In order to examine the adsorbed phase, the benzene was removed by evaporation and the solid sample transferred to an EPR tube. Alternatively, the solid sample was rinsed with benzene, and the filtrate collected and concentrated by partial evaporation of the solvent. Spectra were recorded at room temperature on a Varian E4 or E115 spectrometer at 9 GHz.

Figure 1 shows spectra obtained when PBN was adsorbed on ZnO containing preadsorbed H$_2$ (trace a) and D$_2$ (trace b). The spectra are poorly resolved, but show seven lines in the case of H$_2$ and six for D$_2$. Examination of the solution spectra ob-
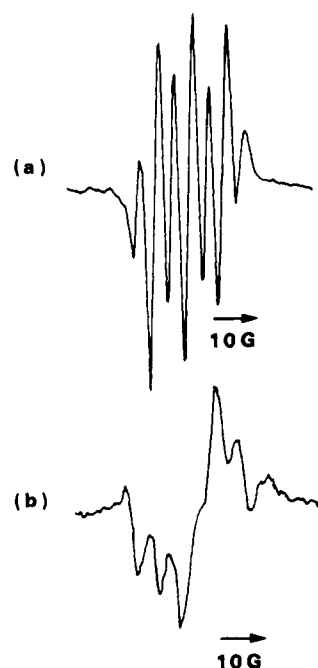

Figure 1. EPR spectra of ZnO containing (a) adsorbed H$_2$ and (b) adsorbed D$_2$ after adsorption of PBN from benzene solution.